AAS 15-250

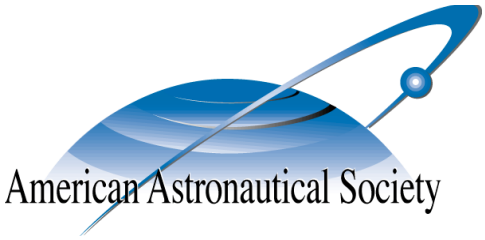

American Institute of
Aeronautics and Astronautics

AN INSTANTANEOUS QUADRATIC POWER OPTIMAL ATTITUDE-TRACKING CONTROL POLICY FOR N-CMG SYSTEMS

Daniel P. Lubey and Hanspeter Schaub

University of Colorado, Boulder, CO, 80309, USA

AAS/AIAA Spaceflight Mechanics Meeting

Williamsburg, Virginia **January 11–15, 2015**

AAS Publications Office, P.O. Box 28130, San Diego, CA 92198

(Preprint) AAS 15-250

AN INSTANTANEOUS QUADRATIC POWER OPTIMAL ATTITUDE-TRACKING CONTROL POLICY FOR N-CMG SYSTEMS

Daniel P. Lubey* **and Hanspeter Schaub†**
University of Colorado, Boulder, CO, 80309, USA

This paper develops an attitude reference tracking control policy that is optimized with respect to the instantaneous power usage for a spacecraft with N Control Moment Gyroscopes (CMGs). Along with the derivation of this control policy, this paper develops the equations of motion for such a system and the control policy is proven to be globally asymptotically stable in both attitude and attitude rate tracking. A numerical simulation is provided to show the power-optimal tracking law performance compared to other control laws such as the minimum norm law for attitude tracking applications.

INTRODUCTION

Attitude control aboard a spacecraft is done in one of two ways: 1) using external forces to torque the vehicle into a desired orientation (thrusters, magnetic torque rods, etc.), and 2) using internal torques to reorient the system (Reactions Wheels [RWs], Control Moment Gyroscopes [CMGs], etc.). In the latter case, internal power is used to operate these momentum management devices. Spacecraft power must be managed properly and preserved, because missions can only persist as long as a power source is available. As such, a minimum power policy for operating these devices is desired.

Optimization with respect to attitude control laws with internal momentum exchange devices has been approached from many different angles including time minimization,[1,2] control minimization,[3] singularity avoidance,[4,5] device orientation,[6,7] and power minimization.[8,9] These methods have been devised for RWs, CMGs, and even more exotic systems like Variable Speeds CMGs (VSCMGs)[3,5] and Double Gimbal VSCMGs.[10] Many methods focus on optimizing over an arc of time, but these methods are often quite difficult to implement on board an active spacecraft. An alternative is to develop instantaneous optimal policies that may be solved analytically or (at the most) through simple algebraic iteration methods that do not require costly computations like integration. Such a power optimal policy was derived for RWs by Schaub and Lappas.[11] This RW control policy fully tracks a reference motion (attitude and attitude rate), and if the system includes redundant RWs it optimizes the instantaneous control torques to use the minimum amount of power (quadratically).

While there has been work in power optimal attitude control, most of this work has focused on RW systems. A goal of this work is to expand this to systems where CMGs are the momentum exchange devices. CMGs provide an effective means to reorient a spacecraft for large and small

*Graduate Research Assistant, Aerospace Engineering Sciences, daniel.lubey@colorado.edu
†Professor, Aerospace Engineering Sciences, hanspeter.schaub@colorado.edu

missions alike,[12,13] and especially for missions that cannot include a propellant system it provides controllability necessary to accomplish mission goals. Some work has focused on deriving power optimal control policies for CMG systems,[14] but they do not specifically apply to spacecraft re-orientation problems where the solution may be easily calculated throughout the maneuver. This development seeks a similar goal to Reference 11 (instantaneous power optimal tracking control) only with CMGs as the momentum exchange device rather than RWs.

This paper develops an attitude tracking control, which distributes the CMG gimbal rates such that the instantaneous power usage is optimized. Section reviews the equations of motion for a spacecraft with N-CMG devices. Section outlines a control law that asymptotically tracks a given attitude reference motion. Section develops the new power optimal control tracking law. Section provides a sample attitude tracking simulation in which the minimum norm tracking control law is compared against the power-optimal solution that is derived in this paper. Finally, Section concludes the paper with a summary and some thoughts on how this work may be advanced in further studies.

N-CMG EQUATIONS OF MOTION

This section focuses on the equations of motion for a system with N CMGs, and how those equations are formulated. A full derivation of these equations is provided in Reference 3. First, the discussion focuses on the equations for the spacecraft attitude, followed by the equations for the CMG states (gimbal angles and rates), and then combining those equations into a final convenient form that may be integrated given initial states, system parameters (inertias), external torques, and control inputs (commanded gimbal torques).

Euler's Equations of Motion with N-CMGs

CMGs operate on the principle of conservation of angular momentum. They consist of a constantly rotating disk that is forced to gimbal by a motor torque. While the magnitude of the CMG's angular momentum remains constant (assuming the disk spins at a constant rate), its orientation varies due to the gimbaling, thus the attached spacecraft must alter its attitude states in order to maintain a constant angular momentum vector in the inertial frame for the total system. Generally, three frames are used to define the system: 1) the Principal Body frame (B), which stays aligned with the spacecraft's principal axes; 2) the Gimbal Frames (G), which stay aligned with their respective CMG as it gimbals; and 3) the Wheel Frames (W), which stay aligned with their respective wheel as it rotates. Each CMG has its own G and W frames but the spacecraft has only one body frame of interest (B).

The equations of motion are derived using Euler's Equation in an approach similar to that of Reference 3. First the total angular momentum of the system must be defined as in Eq. (1). This essentially says the system's total angular momentum is the sum of the spacecraft's and each CMG. Taking the time derivative relative to an inertial frame (Eq. (2)), the equations of motion are obtained by setting them equal to the external torque on the system ($\boldsymbol{L}$). As a notational convenience, any

derivative taken with respect to an inertial frame shall be signified with a dot.

$$\boldsymbol{H} = \boldsymbol{H}_B + \sum_{i=1}^{N} (\boldsymbol{H}_{W,i} + \boldsymbol{H}_{G,i}) \tag{1}$$

$$\dot{\boldsymbol{H}} = \dot{\boldsymbol{H}}_B + \sum_{i=1}^{N} \left(\dot{\boldsymbol{H}}_{W,i} + \dot{\boldsymbol{H}}_{G,i} \right) = \boldsymbol{L} \tag{2}$$

Taking all of these derivatives and combining them into a convenient form, the equations of motion for the angular velocity of the body relative to the inertial frame ($\boldsymbol{\omega}$) are obtained as shown in Eqs. (3) - (11). In terms of notation, $[I_S]$ is the body frame inertia matrix of the spacecraft, which includes all rigid components (i.e. does not account for rotation of the gimbals) as well as the inertia terms that result from the CMGs being offset from the spacecraft center of mass as these are constant in the body frame. $\hat{g}_{s,i}$, $\hat{g}_{t,i}$, and $\hat{g}_{g,i}$ define the spin, transverse, and gimbal axes of the i^{th} CMG, respectively. $\omega_{s,i}$, $\omega_{t,i}$, and $\omega_{g,i}$ represent the components of the body angular velocity projected onto these directions, respectively. $[I_{G,i}]$ represents the inertia of the gimbal about its center of mass with $I_{G_{s,i}}$, $I_{G_{t,i}}$, and $I_{G_{g,i}}$ representing the principal inertias along the spin, transverse, and gimbal axes. γ_i represents the gimbal orientation about the gimbal axis since the inertias are written in the body frame. Ω_i is the wheel rotation rate of the i^{th} CMG, which is assumed to be constant for CMG analysis. The J inertias are the combined gimbal and wheel inertias along the directions indicated by the subscripts.

$$[I]\dot{\boldsymbol{\omega}}_{B/N} = -\boldsymbol{\omega}_{B/N} \times [I]\boldsymbol{\omega}_{B/N} - G_s\boldsymbol{\tau}_s - G_t\boldsymbol{\tau}_t - G_g\boldsymbol{\tau}_g + \boldsymbol{L} \tag{3}$$

$$[I] = [I_S] + \sum_{i=1}^{N} [J_i] \tag{4}$$

$$[J_i] = [I_{Gi}] + [I_{Wi}] \tag{5}$$

$$G_s = \begin{bmatrix} \hat{g}_{s,1} & \dots & \hat{g}_{s,N} \end{bmatrix} \tag{6}$$

$$G_t = \begin{bmatrix} \hat{g}_{t,1} & \dots & \hat{g}_{t,N} \end{bmatrix} \tag{7}$$

$$G_g = \begin{bmatrix} \hat{g}_{g,1} & \dots & \hat{g}_{g,N} \end{bmatrix} \tag{8}$$

$$\boldsymbol{\tau}_s = \langle \boldsymbol{J}_s - \boldsymbol{J}_t + \boldsymbol{J}_g \rangle \langle \boldsymbol{\omega}_t \rangle \dot{\boldsymbol{\gamma}} \tag{9}$$

$$\boldsymbol{\tau}_t = \left(\langle \boldsymbol{J}_s - \boldsymbol{J}_t - \boldsymbol{J}_g \rangle \langle \boldsymbol{\omega}_s \rangle + \langle \boldsymbol{J}_s \rangle \langle \boldsymbol{\Omega} \rangle \right) \dot{\boldsymbol{\gamma}} + \langle \boldsymbol{J}_s \rangle \langle \boldsymbol{\omega}_g \rangle \boldsymbol{\Omega} \tag{10}$$

$$\boldsymbol{\tau}_g = \langle \boldsymbol{J}_g \rangle \ddot{\boldsymbol{\gamma}} - \langle \boldsymbol{J}_s \rangle \langle \boldsymbol{\omega}_t \rangle \boldsymbol{\Omega} \tag{11}$$

In the above expressions, the following notational definitions in Eqs. (12) and (13) are used. This puts the equations in a compact vector form by assembling CMG values ($J_{s,i}$, $J_{t,i}$, $J_{g,i}$, $\omega_{s,i}$, $\omega_{t,i}$, $\omega_{g,i}$, Ω_i, γ_i, $\dot{\gamma}_i$, and $\ddot{\gamma}_i$) into vector and matrix forms. In this form, the notational equivalencies in Eqs. (14) - (16) exist.

$$\boldsymbol{x} = \begin{bmatrix} x_1 & \dots & x_N \end{bmatrix}^T \tag{12}$$

$$\langle \boldsymbol{x} \rangle = \text{diag}(x_i) \tag{13}$$

$$\boldsymbol{\omega}_s = G_s^T \boldsymbol{\omega} \tag{14}$$

$$\boldsymbol{\omega}_t = G_t^T \boldsymbol{\omega} \tag{15}$$

$$\boldsymbol{\omega}_g = G_g^T \boldsymbol{\omega} \tag{16}$$

These equations make the assumption that the wheel spin axis inertia dominates the gimbal spin axis inertia such that $I_{G_{s,i}} + I_{W_{s,i}} \approx I_{W_{s,i}}$. The gimbal frame unit vectors must also be expressed in the body frame, and the $[J_i]$ must be rotated to the body frame in Eq. (4). The wheel is also assumed to be symmetric about its rotation axis so that the same inertia value may be used for the transverse and gimbal directions. It should be noted that the gimbal axes are fixed with respect to the body frame by definition, and the other spin and transverse axes are dined simply by the gimbal angle as defined in Eq. (17).

$$\hat{g}_{s,i}(t) = \cos(\gamma_i(t) - \gamma_i(t_0))\hat{g}_{s,i}(t_0) + \sin(\gamma_i(t) - \gamma_i(t_0))\hat{g}_{t,i}(t_0) \tag{17a}$$

$$\hat{g}_{t,i}(t) = \sin(\gamma_i(t) - \gamma_i(t_0))\hat{g}_{s,i}(t_0) + \cos(\gamma_i(t) - \gamma_i(t_0))\hat{g}_{t,i}(t_0) \tag{17b}$$

$$\hat{g}_{g,i}(t) = \hat{g}_{g,i}(t_0) \tag{17c}$$

Gimbal Torque

The above equations of motion only solve for the body rotation rates. The CMG states also need equations of motion in order to fully define the system. Gimbal torques provide these equations. In the derivation of the previous equations the wheel and gimbal angular momenta rates were computed. Equating the sum of the wheel and gimbal angular momenta to an external torque, and noting that an actuated gimbal motor torque provides the gimbal axis torque the gimbal torque is found as defined in Eq. (18). This torque is presented as a column array with the i^{th} component representing the gimbal torque on the i^{th} CMG as defined by Eq. (12).

$$\boldsymbol{u}_g = \langle \boldsymbol{J}_g \rangle G_g^T \dot{\boldsymbol{\omega}} + \langle \boldsymbol{J}_g \rangle \ddot{\boldsymbol{\gamma}} - \left[\langle \boldsymbol{J}_s - \boldsymbol{J}_t \rangle \langle \boldsymbol{\omega}_s \rangle + \langle \boldsymbol{J}_s \rangle \langle \boldsymbol{\Omega} \rangle \right] \boldsymbol{\omega}_t \tag{18}$$

It should be noted that gimbal accelerations and gimbal rates are sufficient to define the equations of motion for the CMGs, but the equations presented above allow for a more realistic implementation since torques are commanded rather than gimbal accelerations.

Full Equations of Motion

The system as defined has 3+2N states: (1) 3 for angular rate of the spacecraft, (2) N gimbal angles, and (3) N gimbal rates. Additionally, an attitude description would be required (especially if external torques are attitude dependent). The state vector without the attitude description is defined in Eq. (19).

$$\boldsymbol{Z} = \begin{bmatrix} \boldsymbol{\omega}^T & \boldsymbol{\gamma}^T & \dot{\boldsymbol{\gamma}}^T \end{bmatrix}^T \tag{19}$$

Euler's Equations for an N-CMG system are rewritten in Eqs. (20) - (23). In this form, they are written linearally in terms of the state rates, so that the rates may be solved simultaneously when combined with the other equations of motion.

$$[I]\dot{\boldsymbol{\omega}} + A_{\ddot{\gamma}} \ddot{\boldsymbol{\gamma}} = -\boldsymbol{\omega} \times [I]\boldsymbol{\omega} - A_{\dot{\gamma}} \dot{\boldsymbol{\gamma}} - A_{\Omega} \boldsymbol{\Omega} + \boldsymbol{L} \tag{20}$$

$$A_{\ddot{\gamma}} = G_g \langle \boldsymbol{J}_g \rangle \tag{21}$$

$$A_{\dot{\gamma}} = G_s(\langle \boldsymbol{J}_s \rangle - \langle \boldsymbol{J}_t \rangle + \langle \boldsymbol{J}_g \rangle)\langle \boldsymbol{\omega}_t \rangle + G_t \left[(\langle \boldsymbol{J}_s \rangle - \langle \boldsymbol{J}_t \rangle - \langle \boldsymbol{J}_g \rangle)\langle \boldsymbol{\omega}_s \rangle + \langle \boldsymbol{J}_s \rangle \langle \boldsymbol{\Omega} \rangle \right] \tag{22}$$

$$A_{\Omega} = G_t \langle \boldsymbol{J}_s \rangle \langle \boldsymbol{\omega}_g \rangle - G_g \langle \boldsymbol{J}_s \rangle \langle \boldsymbol{\omega}_t \rangle \tag{23}$$

Similarly, the gimbal torque equation is rewritten in a linear form in Eqns. 24 - 26.

$$C_{\dot{\omega}}\dot{\boldsymbol{\omega}} + C_{\ddot{\gamma}}\ddot{\boldsymbol{\gamma}} = \boldsymbol{u}_g + \left[\langle \boldsymbol{J}_s - \boldsymbol{J}_t\rangle\langle\boldsymbol{\omega}_s\rangle + \langle \boldsymbol{J}_s\rangle\langle\boldsymbol{\Omega}\rangle\right]\boldsymbol{\omega}_t \tag{24}$$

$$C_{\dot{\omega}} = \langle \boldsymbol{J}_g\rangle G_g^T \tag{25}$$

$$C_{\ddot{\gamma}} = \langle \boldsymbol{J}_g\rangle \tag{26}$$

These new equation forms allow us to rewrite the equations of motion in a linear form as shown in Eqs. (27) - (29). This version just requires a matrix inverse in order to solve. It is a more intuitive form of the equations too. It allows the user to arbitrarily set N gimbal torques (the actual control variable) during a numerical integration scheme. As will be explored in the following section, the gimbal torques are chosen indirectly through a tracking control which uses gimbal rates as the control variable.

$$M\dot{\boldsymbol{Z}} = \boldsymbol{F} \tag{27}$$

$$M = \begin{bmatrix} [I] & 0_{3xN} & A_{\dot{\gamma}} \\ 0_{3xN} & I_{NxN} & 0_{NxN} \\ C_{\dot{\omega}} & 0_{NxN} & C_{\dot{\gamma}} \end{bmatrix} \tag{28}$$

$$\boldsymbol{F} = \begin{bmatrix} -\boldsymbol{\omega}\times[I]\boldsymbol{\omega} - A_{\dot{\gamma}}\dot{\boldsymbol{\gamma}} - A_{\Omega}\boldsymbol{\Omega} + \boldsymbol{L} \\ \dot{\boldsymbol{\gamma}} \\ \boldsymbol{u}_g + \left[\langle \boldsymbol{J}_s - \boldsymbol{J}_t\rangle\langle\boldsymbol{\omega}_s\rangle + \langle \boldsymbol{J}_s\rangle\langle\boldsymbol{\Omega}\rangle\right]\boldsymbol{\omega}_t \end{bmatrix} \tag{29}$$

As mentioned, an attitude description would be included as states in order to fully describe the system for a tracking problem (such as presented in this paper). This numerical simulations presented here integrate in Euler Parameters and use Modified Rodriguez Parameters (MRPs) for the tracking control, but really any attitude description could be implemented. The differential kinematic equations of motion for the Euler Parameters are:

$$\dot{\boldsymbol{\beta}} = \begin{bmatrix} \dot{\beta}_0 \\ \dot{\beta}_1 \\ \dot{\beta}_2 \\ \dot{\beta}_3 \end{bmatrix} = \frac{1}{2}\begin{bmatrix} \beta_0 & -\beta_1 & -\beta_2 & -\beta_3 \\ \beta_1 & \beta_0 & -\beta_3 & \beta_2 \\ \beta_2 & \beta_3 & \beta_0 & -\beta_1 \\ \beta_3 & -\beta_2 & \beta_1 & \beta_0 \end{bmatrix}\begin{bmatrix} 0 \\ \omega_1 \\ \omega_2 \\ \omega_3 \end{bmatrix} \tag{30}$$

This fully defines the equations of motion for an N-CMG system. The next step is to understand how to best choose our control variable to achieve our control goal - tracking a given reference attitude motion. This is discussed in the next section.

REFERENCE ATTITUDE TRACKING CONTROL LAW

This section reviews a MRP-based infinite horizon control strategy that asymptotically tracks a given reference motion. The control developed in this section is the same as developed in Schaub and Lappas.[11] The power-optimal guidance strategy developed in this paper is not tied to this particular attitude control law. Rather, any CMG-attitude control strategy will lead to the same gimbal rate control constraint formulation.

The control parameters of interest are the gimbal rates of the N-CMGs. Gimbal rates cannot be controlled instantaneously in a real implementation, so an additional gimbal acceleration-based sub-servo loop is used to converge onto the desired gimbal rates of a CMG attitude steering law.

Tracking Control

This tracking control is obtained using Lyapunov analysis. The positive definite, radially unbounded, and continuously differentiable Lyapunov function is expressed in Eq. (31). $\delta\boldsymbol{\omega}$ is defined as the rotation rate of the body frame with respect to the reference frame (the desired orientation). Similarly, $\delta\boldsymbol{\sigma}$ is defined as the MRP definition of the attitude of the body frame with respect to the reference frame. The goal is to find a control that drives both of these measures to zero.

$$V(\delta\boldsymbol{\sigma}, \delta\boldsymbol{\omega}) = \frac{1}{2}\delta\boldsymbol{\omega}^T[I]\delta\boldsymbol{\omega} + 2K\ln(1 + \delta\boldsymbol{\sigma}^T\delta\boldsymbol{\sigma}) \tag{31}$$

Taking the derivative of this Lyapunov function the result in Eq. (32) is obtained. Next, its value is set to a negative semi-definite function, and then the function is solved for the control variable. Although the rate is only negative semi-definite, application of the LaSalle Invariance Principle[15] or the Mukherjee-Chen Theorem[16] will show that the resulting control is globally asymptotically stable.

$$\dot{V}(\delta\boldsymbol{\sigma}, \delta\boldsymbol{\omega}) = \delta\boldsymbol{\omega}^T\left([I]\frac{^B\mathrm{d}(\delta\boldsymbol{\omega})}{\mathrm{d}t} + \frac{1}{2}\frac{^B\mathrm{d}}{\mathrm{d}t}(I)\,\delta\boldsymbol{\omega} + K\delta\boldsymbol{\sigma}\right) = -\delta\boldsymbol{\omega}^T[P]\delta\boldsymbol{\omega} \tag{32}$$

Rearranging the Lyapunov rate the convergence dynamics equation is obtained as shown in Eq. (33). Rearranging the equation results in the form laid out in Eqs. (34) - (41). Tracking control is guaranteed when satisfying Eq. (34). The CMG dynamics are controlled by actuators, so the gimbal rates may be used as the control variable. The gimbal acceleration and gimbal rate cannot be controlled independently since they are related by a time derivative, so the gimbal rate is controlled alone since it makes for a much more efficient momentum exchange device - controlling the gimbal acceleration would result in reaction wheel-like behavior. For convergence, K must be a positive scalar and $[P]$ must be a symmetric positive definite matrix.

$$[I]\frac{^B\mathrm{d}\delta\boldsymbol{\omega}}{\mathrm{d}t} = -\frac{1}{2}\frac{^B\mathrm{d}}{\mathrm{d}t}(I)\,\delta\boldsymbol{\omega} - K\delta\boldsymbol{\sigma} - [P]\delta\boldsymbol{\omega} = [I]\dot{\boldsymbol{\omega}} - [I](\dot{\boldsymbol{\omega}}_r - [\tilde{\omega}]\boldsymbol{\omega}_r) \tag{33}$$

$$[D]\dot{\boldsymbol{\gamma}} + [B]\ddot{\boldsymbol{\gamma}} = \boldsymbol{L}_r \tag{34}$$

$$[B] = G_g\langle\boldsymbol{J}_g\rangle \tag{35}$$

$$[D] = [D1] - [D2] + [D3] + [D4] \tag{36}$$

$$[D1] = \left(G_t\left(\langle\boldsymbol{\Omega}\rangle + \frac{1}{2}\langle\boldsymbol{\omega}_s\rangle\right) + \frac{1}{2}G_s\langle\boldsymbol{\omega}_t\rangle\right)\langle\boldsymbol{J}_s\rangle \tag{37}$$

$$[D2] = \frac{1}{2}\left(G_s\langle\boldsymbol{\omega}_t\rangle + G_t\langle\boldsymbol{\omega}_s\rangle\right)\langle\boldsymbol{J}_t\rangle \tag{38}$$

$$[D3] = \left(G_s\langle\boldsymbol{\omega}_t\rangle - G_t\langle\boldsymbol{\omega}_s\rangle\right)\langle\boldsymbol{J}_t\rangle \tag{39}$$

$$[D4] = \frac{1}{2}\left(G_s\langle G_t^T\boldsymbol{\omega}_r\rangle + G_t\langle G_s^T\boldsymbol{\omega}_r\rangle\right)\left(\langle\boldsymbol{J}_s\rangle - \langle\boldsymbol{J}_t\rangle\right) \tag{40}$$

$$\boldsymbol{L}_r = K\delta\boldsymbol{\sigma} + [P]\delta\boldsymbol{\omega} + \boldsymbol{L} - [\tilde{\omega}][I]\boldsymbol{\omega} - [I](\dot{\boldsymbol{\omega}}_r - [\tilde{\omega}]\boldsymbol{\omega}_r) - \left(G_t\langle\boldsymbol{J}_s\rangle\langle\boldsymbol{\omega}_g\rangle - G_g\langle\boldsymbol{J}_s\rangle\langle\boldsymbol{\omega}_t\rangle\right)\boldsymbol{\Omega} \tag{41}$$

For the CMG gimbal rate steering-law development, it is generally assumed that the $[B]\ddot{\boldsymbol{\gamma}}$ term is negligible.

$$[D]\dot{\boldsymbol{\gamma}} \approx \boldsymbol{L}_r \tag{42}$$

Next, the equation is rearranged to yield the desired gimbal rates. If N = 3 and the CMGs are not in gimbal lock (singular configuration), then a unique solution exists. Otherwise, a greater number of CMGs yields a null space that offers an infinity of solutions, which provides room for optimization. Generally a minimum norm inverse is used to solve for the desired gimbal rates.

$$\dot{\boldsymbol{\gamma}}_{MN} = [D]^T \left([D][D]^T\right)^{-1} \boldsymbol{L}_r \tag{43}$$

Implementing these desired rates requires an additional control loop as explained in the following subsection.

Subservo Control

Motor Torques cannot instantaneously implement desired gimbal rates, so a subservo control loop is used to converge onto these desired rates. A similar Lyapunov analysis is used to obtain the control law shown in Eq. (47). The subscript "d" implies desired values. The desired gimbal accelerations must be determined numerically, or they may be ignored if a feedforward term is not important. For convergence $K_{\dot{\gamma}}$ must be a positive scalar.

$$\Delta\dot{\boldsymbol{\gamma}} = \dot{\boldsymbol{\gamma}} - \dot{\boldsymbol{\gamma}}_d \tag{44}$$

$$V(\Delta\dot{\boldsymbol{\gamma}}) = \frac{1}{2}\Delta\dot{\boldsymbol{\gamma}}^T\Delta\dot{\boldsymbol{\gamma}} \tag{45}$$

$$\dot{V}(\Delta\dot{\boldsymbol{\gamma}}) = -\Delta\dot{\boldsymbol{\gamma}}^T\Delta\ddot{\boldsymbol{\gamma}} = -K_{\dot{\gamma}}\Delta\dot{\boldsymbol{\gamma}}^T\Delta\dot{\boldsymbol{\gamma}} \tag{46}$$

$$\ddot{\boldsymbol{\gamma}} = -K_{\dot{\gamma}}(\dot{\boldsymbol{\gamma}} - \dot{\boldsymbol{\gamma}}_d) + \ddot{\boldsymbol{\gamma}}_d \tag{47}$$

This fully defines our MRP-based asymptotic reference tracking control law. As mentioned, when a system contains redundant CMGs (N >3) it offers room for control optimization. In the next section the focus will be on deriving the central algorithm of this paper - a power optimal MRP-based asymptotic reference tracking control law.

POWER OPTIMAL CONTROL POLICY

To develop a power optimal control law it is necessary to first understand how power is related to the implemented control. Using the Work-Energy Principle, the power equation for an N-CMG spacecraft is shown in Eq. (48). The power is basically a function of the two rotation rates associated with a CMG (wheel rate and gimbal rate) and the torques associated with these rates. The gimbal torque is controlled for a CMG, but the spin torque is not actuated (it just maintains constant wheel speed), though it is a simplified version of the torque that a Variable Speed CMG (VSCMG) would need to impart to adjust the wheel speed. For this analysis it is assumed that the external torque is effectively zero (or at least independent of the desired gimbal rate).

$$P = \boldsymbol{\omega}^T\boldsymbol{L} + \sum_{i=1}^{N}\left(\Omega_i u_{s,i} + \dot{\gamma}_i u_{g,i}\right) = \boldsymbol{\omega}^T\boldsymbol{L} + \boldsymbol{\Omega}^T\boldsymbol{u}_s + \dot{\boldsymbol{\gamma}}^T\boldsymbol{u}_g \tag{48}$$

$$\boldsymbol{u}_s = \langle \boldsymbol{J}_s\rangle G_s^T\dot{\boldsymbol{\omega}} + \langle \boldsymbol{J}_s\rangle\langle\boldsymbol{\omega}_t\rangle\dot{\boldsymbol{\gamma}} \tag{49}$$

This equation for power includes a term that we cannot instantaneously control, and that has no bearing on the control torques ($\boldsymbol{\omega}^T\boldsymbol{L}$). Additionally, this equation sums over the powers from each

CMG to get a total value for the system. It is assumed that there is no system in place to reclaim power from the system when a negative power occurs (e.g. flywheel), so even when power reads as negative the CMG must output energy. As such, it is necessary to adapt our power cost function to be more meaningful to this problem. Instead of minimizing the power equation above, an analog is used that removes the term with no control torque, and sums over the squares of the powers from the individual CMGs. This will ensure that the focus is on minimizing the magnitude of each of these powers rather than a sum where a CMG with a strong negative power can negate the positive powers from the other CMGs. This power analogous function is defined in Eq. (50).

$$\begin{gathered}\mathcal{J}(\dot{\boldsymbol{\gamma}}) = \tfrac{1}{2}\mathcal{P}^2 = \tfrac{1}{2}\boldsymbol{P}^T\boldsymbol{P} \\ \boldsymbol{P} = \left(\langle\boldsymbol{\Omega}\rangle\langle\boldsymbol{J}_s\rangle G_s^T + \langle\dot{\boldsymbol{\gamma}}\rangle\langle\boldsymbol{J}_g\rangle G_g^T\right)\dot{\boldsymbol{\omega}} + \left(\langle\boldsymbol{J}_g\rangle\langle\ddot{\boldsymbol{\gamma}}\rangle - \langle\boldsymbol{J}_s - \boldsymbol{J}_t\rangle\langle\boldsymbol{\omega}_s\rangle\langle\boldsymbol{\omega}_t\rangle\right)\dot{\boldsymbol{\gamma}}\end{gathered} \tag{50}$$

Other than minimizing this cost, it is important to also ensure that the control follows the tracking law, and that it also does not require unachievable gimbal rates. As such, the equality constraint defined in Eq. (51) and the inequality constraint defined in Eq. (52) are enforced. It should be noted that the max gimbal rate needs be set equal to or larger than the minimum norm solution since by definition this is the smallest gimbal rate that adheres to the tracking control law.

$$h(\dot{\boldsymbol{\gamma}}) = [D]\dot{\boldsymbol{\gamma}} - \boldsymbol{L}_r = \boldsymbol{0} \tag{51}$$

$$g(\dot{\boldsymbol{\gamma}}) = \dot{\boldsymbol{\gamma}}^T\dot{\boldsymbol{\gamma}} - \dot{\gamma}_{\text{max}}^2 \leq \boldsymbol{0} \tag{52}$$

Note that Eq. (51) is written to account for a general CMG steering law that requires $[D]\dot{\boldsymbol{\gamma}} = \boldsymbol{L}_r$, and the following general developments are not specific to the MRP-based attitude tracking control employed in this study.

From this point we will pursue a solution that minimizes this power analogous function while adhering to these two constraints. The problem is nonlinear in the control variable, thus an analytical solution for N-CMGs cannot be obtained; however, for a system with 4 CMGs the problem can be solved explicitly. Both of these solutions will be explored in the following discussion.

Optimization for a System with N CMGs

Minimization of this power-analogous cost function with an equality constraint and an inequality constraint is accomplished via application of the Karush-Kuhn-Tucker (KKT) conditions.[17] To apply these conditions it is necessary to define the Lagrangian function in Eq. (53).

$$\mathcal{L}(\dot{\boldsymbol{\gamma}}, \boldsymbol{\lambda}, \mu) = \frac{1}{2}\mathcal{P}(\dot{\boldsymbol{\gamma}})^2 + \boldsymbol{\lambda}^T h(\dot{\boldsymbol{\gamma}}) + \mu g(\dot{\boldsymbol{\gamma}}) \tag{53}$$

The KKT conditions provide three necessary conditions for optimality (stationary, equality, and inequality conditions) as defined in Eqs. (54) -(56). The Lagrange multiplier on the inequality constraint (μ) can be viewed as a switching function - when exploring solutions in the domain where the constraint is negative the multiplier is zero, and on the boundary the constraint acts as an equality constraint. This is summarized in Eq. (56).

$$\frac{\partial\mathcal{L}(\dot{\boldsymbol{\gamma}}, \boldsymbol{\lambda}, \mu)}{\partial\dot{\boldsymbol{\gamma}}}^T = \frac{1}{2}\nabla\mathcal{P}(\dot{\boldsymbol{\gamma}})^2 + \nabla h(\dot{\boldsymbol{\gamma}})\boldsymbol{\lambda} + \mu\nabla g(\dot{\boldsymbol{\gamma}}) = \boldsymbol{0} \tag{54}$$

$$h(\dot{\boldsymbol{\gamma}}) = \boldsymbol{0} \tag{55}$$

$$\mu g(\dot{\boldsymbol{\gamma}}) = 0, \quad \mu \geq 0 \tag{56}$$

Evaluating each of the partials from Eq. (54) the results in Eqs. (57) - (59) are obtained. The partial of the power-analogous function is nonlinear, thus an explicit solution to this optimization problem cannot be obtained. Linearizing the problem to develop an iterative approach that converges on the nonlinear optimal solution provides a numerical method for solving the problem.

$$\nabla \mathcal{P}(\dot{\boldsymbol{\gamma}})^2 = \frac{\partial \mathcal{P}^2}{\partial \dot{\boldsymbol{\gamma}}}^T = 2 \frac{\partial \boldsymbol{P}}{\partial \dot{\boldsymbol{\gamma}}}^T \boldsymbol{P} \tag{57}$$

$$\nabla h(\dot{\boldsymbol{\gamma}}) = \frac{\partial h(\dot{\boldsymbol{\gamma}})}{\partial \dot{\boldsymbol{\gamma}}}^T = [D]^T \tag{58}$$

$$\nabla g(\dot{\boldsymbol{\gamma}}) = \frac{\partial g(\dot{\boldsymbol{\gamma}})}{\partial \dot{\boldsymbol{\gamma}}}^T = 2\dot{\boldsymbol{\gamma}} \tag{59}$$

When linearizing you cannot have discontinuities in the linearized parameters, thus the solution must be approached in two ways: (1) optimize assuming the solution lies within the inequality constraint, and (if this solution is found to invalidate the inequality constraint) (2) optimize assuming $g(\dot{\boldsymbol{\gamma}})$ is an equality constraint. For the first approach one must completely neglect the impact of the inequality constraint. Because the tracking constraint is linear in the control variable it is not necessary to linearize the Lagrange multiplier - only with respect to the gimbal rates. This linearization is defined with respect to a nominal gimbal rate ($\dot{\boldsymbol{\gamma}}^{(i)}$) as shown in Eq. (60), where the i superscript indicate the values on the i^{th} iteration.

$$\frac{1}{2}\left[\nabla \mathcal{P}^2(\dot{\boldsymbol{\gamma}}^{(i)}) + \nabla^2 \mathcal{P}^2(\dot{\boldsymbol{\gamma}}^{(i)}) \delta\dot{\boldsymbol{\gamma}}^{(i)}\right] + [D]^T \boldsymbol{\lambda}^{(i)} = \mathbf{0} \tag{60}$$

Solving for the deviation in the gimbal rate from the nominal rate one can plug this into Eq. (55) to solve for the Lagrange multiplier in terms of the gimbal rate, which can in turn be used to explicitly solve for the linearized gimbal rate. The results of this process are defined in Eqs. (61) and (62). This process should be iterated until the gimbal rate update is less than a set tolerance ($||\delta\dot{\boldsymbol{\gamma}}^{(i)}||_\infty < \Delta$). In practice, starting with the minimum norm solution as the initial guess for this iterative root finder has been found to be effective at solving the problem.

$$\begin{aligned} \dot{\boldsymbol{\gamma}}^{(i+1)} =& \dot{\boldsymbol{\gamma}}^{(i)} + \delta\dot{\boldsymbol{\gamma}}^{(i)} \\ =& \dot{\boldsymbol{\gamma}}^{(i)} - \left(\nabla^2 \mathcal{P}^2(\dot{\boldsymbol{\gamma}}^{(i)})\right)^{-1} \left[2[D]^T \boldsymbol{\lambda}^{(i)} + \nabla \mathcal{P}^2(\dot{\boldsymbol{\gamma}}^{(i)})\right] \end{aligned} \tag{61}$$

$$\begin{aligned} \boldsymbol{\lambda}^{(i)} =& -\frac{1}{2}\left([D]\left(\nabla^2 \mathcal{P}^2(\dot{\boldsymbol{\gamma}}^{(i)})\right)^{-1}[D]^T\right)^{-1} \\ & \times \left[[D]\left(\nabla^2 \mathcal{P}^2(\dot{\boldsymbol{\gamma}}^{(i)})\right)^{-1} \nabla \mathcal{P}^2(\dot{\boldsymbol{\gamma}}^{(i)}) - \left[[D]\dot{\boldsymbol{\gamma}}^{(i)} - \boldsymbol{L}_r\right]\right] \end{aligned} \tag{62}$$

If the solution to this problem does not satisfy the inequality constraint, the next step is to reoptimize now assuming this constraint to be an equality constraint. Because this constraint is nonlinear

in the gimbal rate it is necessary to linearize its Lagrange multiplier. This linearization is defined in Eqs. (63) and (64).

$$\begin{aligned}\frac{1}{2}\left[\nabla\mathcal{P}^2(\dot{\boldsymbol{\gamma}}^{(i)})+\nabla^2\mathcal{P}^2(\dot{\boldsymbol{\gamma}}^{(i)})\delta\dot{\boldsymbol{\gamma}}^{(i)}\right]+[D]^T\boldsymbol{\lambda}^{(i)} \\ +\left[\mu^{(i)}\nabla g(\dot{\boldsymbol{\gamma}}^{(i)})+2\mu^{(i)}\delta\dot{\boldsymbol{\gamma}}^{(i)}+\nabla g(\dot{\boldsymbol{\gamma}}^{(i)})\delta\mu^{(i)}\right]=\mathbf{0}\end{aligned} \tag{63}$$

$$\left(\dot{\boldsymbol{\gamma}}^{(i)^T}\dot{\boldsymbol{\gamma}}^{(i)}-\dot{\gamma}_{\text{max}}^2\right)+2\dot{\boldsymbol{\gamma}}^{(i)^T}\delta\dot{\boldsymbol{\gamma}}^{(i)}=0 \tag{64}$$

Solving these equations along with the tracking equality constraint results in the linear solutions in Eqs. (65) - (69). Again, this process should be iterated until the desired level of convergence is achieved in both the gimbal rates and the inequality constraint Lagrange multiplier.

$$\begin{aligned}\dot{\boldsymbol{\gamma}}^{(i+1)}=&\dot{\boldsymbol{\gamma}}^{(i)}+\delta\dot{\boldsymbol{\gamma}}^{(i)} \\ =&\dot{\boldsymbol{\gamma}}^{(i)}-\left[\frac{1}{2}\nabla^2\mathcal{P}^2(\dot{\boldsymbol{\gamma}}^{(i)})+2\mu^{(i)}I_{NxN}\right]^{-1}\left(\frac{1}{2}\nabla\mathcal{P}^2(\dot{\boldsymbol{\gamma}}^{(i)})+\mu^{(i)}\nabla g(\dot{\boldsymbol{\gamma}}^{(i)})\right. \\ &\left.+[D]^T\boldsymbol{\lambda}^{(i)}+\nabla g(\dot{\boldsymbol{\gamma}}^{(i)})\delta\mu^{(i)}\right)\end{aligned} \tag{65}$$

$$\mu^{(i+1)}=\mu^{(i)}+\delta\mu^{(i)} \tag{66}$$

$$\begin{bmatrix}\boldsymbol{\lambda}^{(i)}\\ \delta\mu^{(i)}\end{bmatrix}=Q^{-1}\boldsymbol{T} \tag{67}$$

$$Q=\begin{bmatrix}[D]\left[\frac{1}{2}\nabla^2\mathcal{P}^2(\dot{\boldsymbol{\gamma}}^{(i)})+2\mu^{(i)}I_{NxN}\right]^{-1}\\ 2\dot{\boldsymbol{\gamma}}^{(i)^T}\left[\frac{1}{2}\nabla^2\mathcal{P}^2(\dot{\boldsymbol{\gamma}}^{(i)})+2\mu^{(i)}I_{NxN}\right]^{-1}\end{bmatrix}\begin{bmatrix}[D]^T & \nabla g(\dot{\boldsymbol{\gamma}}^{(i)})\end{bmatrix} \tag{68}$$

$$\begin{aligned}\boldsymbol{T}=&-\begin{bmatrix}[D]\\ 2\dot{\boldsymbol{\gamma}}^{(i)^T}\end{bmatrix}\left[\frac{1}{2}\nabla^2\mathcal{P}^2(\dot{\boldsymbol{\gamma}}^{(i)})+2\mu^{(i)}I_{NxN}\right]^{-1}\left(\frac{1}{2}\nabla\mathcal{P}^2(\dot{\boldsymbol{\gamma}}^{(i)})+\mu^{(i)}\nabla g(\dot{\boldsymbol{\gamma}}^{(i)})\right) \\ &+\begin{bmatrix}[D]\dot{\boldsymbol{\gamma}}^{(i)}-\boldsymbol{L}_r\\ \dot{\boldsymbol{\gamma}}^{(i)^T}\dot{\boldsymbol{\gamma}}^{(i)}-\dot{\gamma}_{max}^2\end{bmatrix}\end{aligned} \tag{69}$$

This method provides a solution that minimizes our power-analogous cost function subject to constraints that ensure the control still tracks the reference motion and does not command too large of gimbal rates. The method works for $N > 3$ CMGs in the system, but must be solved iteratively to obtain a control solution. The next subsection focuses on systems with $N = 4$ CMGs, and how an analytical solution may be obtained for this specific case.

Optimization for a System with Four CMGs

Mechanical redundancy in space based missions helps to prevent missions from early mechanical and electrical failures, thus it is desirable; however, this must be balanced against the added mass and power requirements that redundant systems bring along with them. As such, a typical attitude control system has only 4 momentum exchange devices to provide the minimum amount of redundancy (three are required for complete controllability), and the fourth provides the minimum amount of redundancy (assuming they are arranged properly to avoid gimbal lock). Our focus now is on obtaining an analytical solution to this problem for systems with 4 CMGs, since this would make the algorithm far more practically implementable for a real application.

In the previous method tracking constraints were enforced via a Lagrange multiplier; however, given this is a linear constraint in the control it can be implemented in an alternative manner. The $[D]$ matrix for a system with four CMGs has a defined null space that is one-dimensional. The unit vector that defines this null space ($\hat{n}$) is the unit eigenvector that accompanies the eigenvalue of 0 for the matrix $[D]^T[D]$. If the solution to the gimbal rate is defined as described in Eq. (70), then the gimbal rate satisfies the tracking constraint for any real value of τ. The problem now is to select the parameter τ that minimizes the cost function subject to the defined inequality constraint.

$$\dot{\boldsymbol{\gamma}}(\tau) = \dot{\boldsymbol{\gamma}}_{MN} + \hat{n}\tau \tag{70}$$

To start this optimization process, the cost function is defined in terms of τ as shown in Eqs. (71) - (75).

$$\mathcal{J}(\tau) = \frac{1}{2}\tilde{P}^2 = \frac{1}{2}\boldsymbol{P}_0^T\boldsymbol{P}_0 + \boldsymbol{P}_1^T\boldsymbol{P}_0\tau + \left(\boldsymbol{P}_2^T\boldsymbol{P}_0 + \frac{1}{2}\boldsymbol{P}_1^T\boldsymbol{P}_1\right)\tau^2 + \boldsymbol{P}_2^T\boldsymbol{P}_1\tau^3 + \frac{1}{2}\boldsymbol{P}_2^T\boldsymbol{P}_2\tau^4 \tag{71}$$

$$\boldsymbol{P} = \boldsymbol{P}_0 + \boldsymbol{P}_1\tau + \boldsymbol{P}_2\tau^2 \tag{72}$$

$$\begin{aligned}\boldsymbol{P}_0 = {} & \left(\langle\boldsymbol{\Omega}\rangle\langle\boldsymbol{J}_s\rangle G_s^T + \langle\dot{\boldsymbol{\gamma}}_{MN}\rangle\langle\boldsymbol{J}_g\rangle G_g^T\right)[I]^{-1}\left[-\boldsymbol{\omega}\times[I]\boldsymbol{\omega} - A_{\dot{\gamma}}\dot{\boldsymbol{\gamma}}_{MN} - A_\Omega\boldsymbol{\Omega}\right. \\ & \left. -A_{\ddot{\gamma}}\ddot{\boldsymbol{\gamma}} + \boldsymbol{L}\right] + \left(\langle\boldsymbol{J}_g\rangle\langle\ddot{\boldsymbol{\gamma}}\rangle - \langle\boldsymbol{J}_s - \boldsymbol{J}_t\rangle\langle\boldsymbol{\omega}_s\rangle\langle\boldsymbol{\omega}_t\rangle\right)\dot{\boldsymbol{\gamma}}_{MN}\end{aligned} \tag{73}$$

$$\begin{aligned}\boldsymbol{P}_1 = {} & \left(\langle\boldsymbol{J}_g\rangle\langle\ddot{\boldsymbol{\gamma}}\rangle - \langle\boldsymbol{J}_s - \boldsymbol{J}_t\rangle\langle\boldsymbol{\omega}_s\rangle\langle\boldsymbol{\omega}_t\rangle\right)\hat{n} - \left(\langle\boldsymbol{\Omega}\rangle\langle\boldsymbol{J}_s\rangle G_s^T + \langle\dot{\boldsymbol{\gamma}}_{MN}\rangle\langle\boldsymbol{J}_g\rangle G_g^T\right)[I]^{-1}A_{\dot{\gamma}}\hat{n} \\ & +\langle\hat{n}\rangle\langle\boldsymbol{J}_g\rangle G_g^T[I]^{-1}\left[-\boldsymbol{\omega}\times[I]\boldsymbol{\omega} - A_{\dot{\gamma}}\dot{\boldsymbol{\gamma}}_{MN} - A_\Omega\boldsymbol{\Omega} - A_{\ddot{\gamma}}\ddot{\boldsymbol{\gamma}} + \boldsymbol{L}\right]\end{aligned} \tag{74}$$

$$\boldsymbol{P}_2 = -\langle\hat{n}\rangle\langle\boldsymbol{J}_g\rangle G_g^T[I]^{-1}A_{\dot{\gamma}}\hat{n} \tag{75}$$

This results in a simple 4$^{\text{th}}$ order polynomial defining the cost function. To optimize this and obtain a solution one simply needs to take the derivative of this polynomial and find the zeros of the resulting third order polynomial (Eq. (76)), for which an analytic solution exists.[18] There will be three solutions to this minimization, but only real roots of the derivative that have positive second derivatives (Eq. (77)) can be minimizing solutions. In practice only one of the three roots has been real with a positive second derivative (indicating a unique solution), but if a situation arises where two plausible solutions exist the one that gives a smaller cost function value or provides smaller

commanded gimbal rates (if they are equal in cost) should be selected. It is left as future work to prove the uniqueness of this solution analytically.

$$\frac{d\mathcal{J}(\tau)}{d\tau} = \boldsymbol{P}_1^T \boldsymbol{P}_0 + \left(2\boldsymbol{P}_2^T \boldsymbol{P}_0 + \boldsymbol{P}_1^T \boldsymbol{P}_1\right)\tau + 3\boldsymbol{P}_2^T \boldsymbol{P}_1 \tau^2 + 2\boldsymbol{P}_2^T \boldsymbol{P}_2 \tau^3 = 0 \tag{76}$$

$$\frac{d^2\mathcal{J}(\tau)}{d\tau^2} = \left(2\boldsymbol{P}_2^T \boldsymbol{P}_0 + \boldsymbol{P}_1^T \boldsymbol{P}_1\right) + 6\boldsymbol{P}_2^T \boldsymbol{P}_1 \tau + 6\boldsymbol{P}_2^T \boldsymbol{P}_2 \tau^2 > 0 \tag{77}$$

If the resulting solution does not adhere to the inequality constraint, then the next step is to revaluate using it as a new equality constraint (Eq. (78)) - this equation accounts for the fact that the null vector is orthogonal to the minimum norm solution by definition. This gives a quadratic equation in τ that is guaranteed to have two real solutions given that the maximum gimbal rates are not set lower than the minimum norm solution. You choose the positive or negative root based on which yields a smaller cost function evaluation - this avoids having to solve for a Lagrange multiplier associated with this constraint.

$$\tau^2 + \left(\dot{\boldsymbol{\gamma}}_{MN}^T \dot{\boldsymbol{\gamma}}_{MN} - \dot{\gamma}_{\text{max}}^2\right) = 0 \tag{78}$$

This fully defines our analytical power-optimal solution for systems with 4 CMGs. The method is easily implementable on board a real spacecraft, requiring no integration or solution iteration - just accurate state estimates. For more complex systems, a power-optimal solution for N-CMG systems is also derived. While this solution requires iteration it still provides a control with instantaneous power savings that asymptotically tracks a given reference motion. The following section provides an example of this algorithm at work, and a discussion of how it compares to the minimum norm solution.

NUMERICAL SIMULATIONS

A numerical implementation of this policy is presented in this section. The results from the power optimal policy are compared to the minimum norm solution to provide metrics for how these control policies perform. The minimum power is run at two different levels for the max gimbal rate in order to show how the inequality constraint affects the response. The first case sets the maximum at twice the minimum norm magnitude (MP 2x), and the second case sets it at four times the minimum norm magnitude (MP 4x).The test case presented here involves a spacecraft with 4 CMGs tracking the reference displayed below ($D = \frac{1}{1000sec}$). Simulation parameters are defined in Tables 1 - 4.

$$\boldsymbol{\sigma} = \begin{bmatrix} 2Dt \\ -(Dt)^2 \\ \frac{1}{2}Dt \end{bmatrix} \tag{79}$$

Table 1. System Inertias

Inertia	Value ($kg * m^2$)
$I_{S,1}$	86.215
$I_{S,2}$	85.070
$I_{S,3}$	113.565
J_{s_i}	0.13
J_{t_i}	0.04
J_{g_i}	0.03

Table 2. Initial States

State	Value
$\boldsymbol{\sigma}$	$[0.414, 0.3, 0.2]$
${}^{B}\boldsymbol{\omega}_{B/N}$	$[0.01, 0.05, -0.01]$ rad/s
Ω_i	14.4 rad/s
$\gamma_i(0)$	0 rad
$\dot{\boldsymbol{\gamma}}(0)$	$[0, 0, 0, 0]$ rad/s

Table 3. Initial CMG Orientations

Axis	Values
$G_s(0)$	$\begin{bmatrix} 1 & -1 & 0 & 0 \\ 0 & 0 & 1 & -1 \\ 0 & 0 & 0 & 0 \end{bmatrix}$
$G_t(0)$	$\begin{bmatrix} 0 & 0 & -0.8166 & 0.8166 \\ 0.8166 & -0.8166 & 0 & 0 \\ -0.5771 & -0.5771 & 0.5771 & 0.5771 \end{bmatrix}$
$G_g(0)$	$\begin{bmatrix} 0 & 0 & 0.5771 & -0.5771 \\ 0.5771 & -0.5771 & 0 & 0 \\ 0.8166 & 0.8166 & 0.8166 & 0.8166 \end{bmatrix}$

Table 4. Control Gains

Gain	Value
K	0.2 N*m
$K_{\dot{\gamma}}$	1.5 1/sec
$[P]$	$\begin{bmatrix} 3 & 0 & 0 \\ 0 & 3 & 0 \\ 0 & 0 & 3 \end{bmatrix}$ N*m*sec

Figure 1 shows the convergence of the attitude and attitude rates of the simulation for each control law (Body frame with respect to the Reference motion). It is clear from these results that the two methods perform quite comparably over the entire simulation. At times one performs slightly better than the other, but in general they keep flipping back and forth. This is to be expected since both control policies satisfy the tracking constraint that we derived. Given the same gains, both methods should converge at a comparable rate based on our Lyapunov analysis barring numerical errors in either method. The larger the maximum gimbal rate is set the slower the convergence after 700 seconds, though. As such it might be helpful to switch to the minimum norm solution once the bulk of the convergence has been obtained since power savings are no long a concern at such small torque levels, and the minimum norm solution performs best when subtle changes are needed.

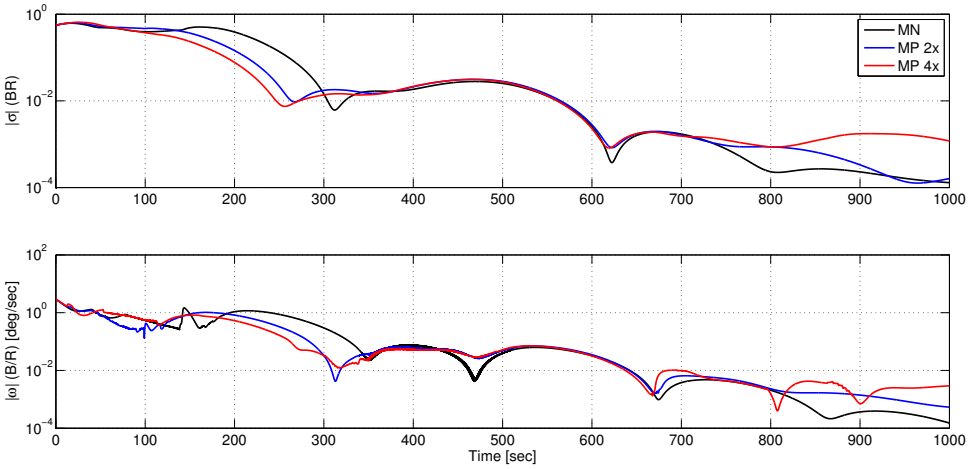

Figure 1. Attitude (top) and Attitude Rate (bottom) Convergence for each Control Law - (MN) Minimum Norm Solution and (MP) Minimum Power Solution.

The desired gimbal rates from all three simulations are summarized in Fig. 2. One might expect the minimum norm solution to have the smallest gimbal rates, but this does not seem to be the case. The highest peak gimbal rates occur for the minimum norm case, and as the maximum allowed gimbal rate is increased that peak diminishes. This is because these control policies are optimal in an instantaneous sense, meaning they provide minimal solutions at the given time for a given set of states and control gains. Since these two solutions create two separate trajectories (with the same

gains, but different states) there is no requirement that one must always provide a minimal gimbal rate or minimum power solution at all times. These optimal behaviors tend to pop out over the course of an entire simulation, but there will be times when the other solution performs better.

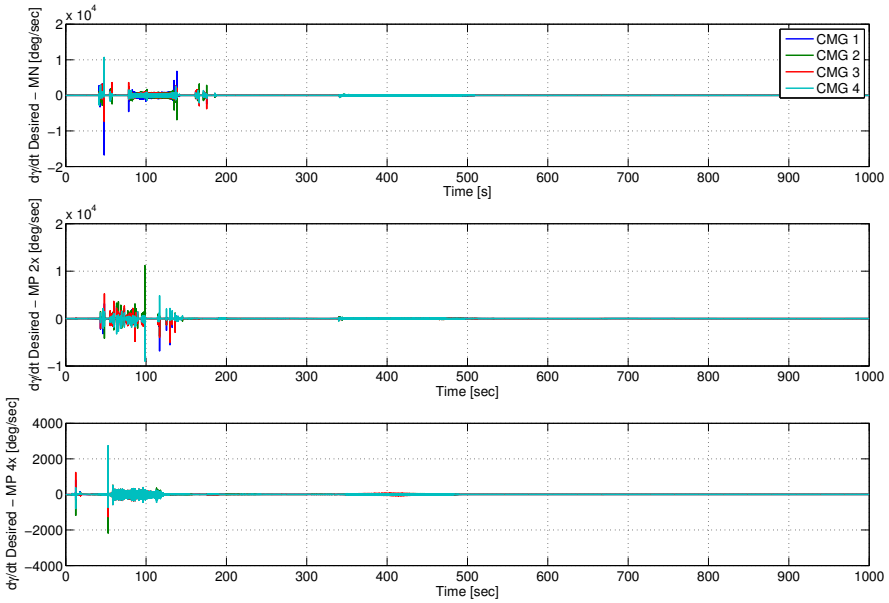

Figure 2. Desired Gimbal Rates for Each Control Law on their Individual Trajectories: (Top) Minimum Norm Solution, (Middle) Minimum Power Solution #1 (MP 2x), and (Bottom) Minimum Power Solution #2 (MP 4x)

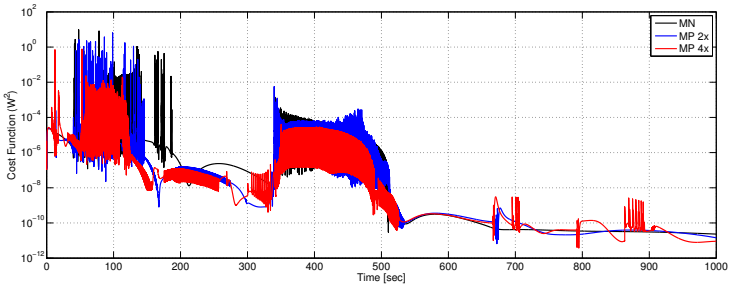

Figure 3. Quadratic Power-Analog for Each Control Law on their Respective Trajectories

Having compared convergence and control results, it is now appropriate to compare performances based on the metric of interest in this paper - the power analogous cost function that was proposed proposed (Eq. (50)). These results are summarized in Fig. 3. It is clear in these results the minimum power solution minimizes our cost function of interest in general, and it provides the best results as the maximum allowed gimbal rate is increased. Its peak power usage is smaller than the minimum norm solution for both cases, and there are periods where it clearly outperforms the minimum norm solution (e.g. between 125 and 325 seconds). There are times when the minimum norm solution performs slightly better(especially in the turbulent periods when compared to the first minimum

power simulation), but this a symptom of the instantaneous nature of the optimization as discussed previously.

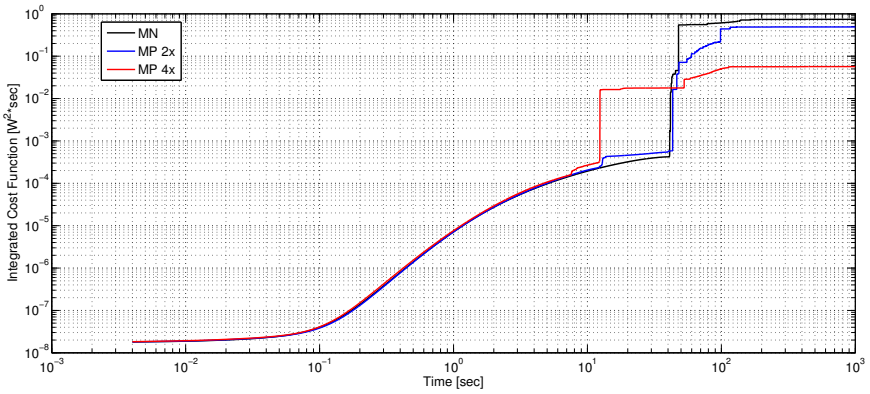

Figure 4. Integrated cost function as a function of time for minimum norm and minimum power simulations.

While this optimization procedure makes no guarantees about minimizing the cost across some duration, this might be expected since it guarantees optimal behavior at each instant. Figure 4 shows the power-analogous cost function integrated with respect to time for all three cases. This integrated cost is similar to an energy metric (though the power was squared to make it positive definite), so it indicates how much energy the torques must impart on the system from the system's power subsystem. These results indicate that over the course of the maneuver the minimum power simulations outperform the minimum norm with a total integrated costs that are 33% less and 92% less than the minimum norm's integrated cost, respectively. Both cases are significant power savings, but the latter is drastic. This demonstrate's this algorithm's ability to save energy while providing comparable tracking performance when compared to the minimum norm solution. Again, by adjusting system parameters such as gains and the maximum allowed gimbal rate magnitude (as demonstrated), it may be possible to find even greater energy savings. Such adjustments should be made prior to beginning any real attitude maneuver.

This simulation has demonstrated both the minimum norm solution, and our custom minimum power solution. It is clear from the results that both methods accurately track a reference motion (at a comparable level between the two methods), and that our solution tends to minimize power usage in the system. This specific example has some turbulent behavior that is likely a symptom of the system approaching gimbal lock. Without this issue we would expect to see smoother behavior in the commanded gimbal rates and the power performance. In general, both methods should be simulated a priori and adjusted via gain selection in order to smooth out performance for actual implementation aboard a spacecraft.

CONCLUSIONS AND FUTURE WORK

This paper fully defined the system of interest through the description of its equations of motion and a globally asymptotically stable tracking control policy. It then addressed the problem at hand by deriving an instantaneous power optimal control policy for systems with redundant Control Moment Gyroscopes (CMGs). This control policy has the same stability guarantees as the original

derivation it just does so in a manner that uses the least amount of power possible given a set of states and gains at the given moment.

Through a numerical simulation a comparison between the performance of this power-optimal policy and a more standard minimum norm solution was made. This revealed that both control policies accurately track a moving reference, and that the optimal power policy minimizes power usage in the system - with ability to yield drastic energy savings over the course of an entire maneuver. There are short periods where the minimum norm solution performs slightly better, but overall the optimal solution performs better. Because these control policies are optimized instantaneously there is no guarantee that the power optimal solution will outperform the minimum norm solution for a given set of gains since they provide convergence via two separate state trajectories. As such both methods should be tested a priori before large attitude maneuvers to determine which is best suited to be implemented and what the gains for the maneuver should be.

In the future one focus is to guarantee minimum power performance over the duration of the simulation. To do this one would need to approach the problem as a time-fixed attitude maneuver where the integral of the power is minimized over the course of the maneuver. This solution will look entirely different than what has been derived here as this paper is an example of parametric optimization whereas performance over the entire trajectory would require functional optimization methods. By generating this type of solution, though, one would be able to implement it at all times without verifying that it performs better over the course of the maneuver. This is balanced by the computational complexity of the solution, so it would valuable to compare this instantaneous policy against an integrated policy in terms of power performance and computational time required to determine which methods are best for real-world application.

REFERENCES

[1] Melton, R.G., *Improved Starting Points for Heuristic Searches in a Time-Optimal Slew-Maneuver Problems*, AIAA/AAS Astrodynamics Specialist Conference, Aug. 2014. doi: 10.2514/6.2014-4298.

[2] Kranton, J. *Minimum-Time Attitude Maneuvers with Control Moment Gyroscopes*, AIAA Journal, Vol. 8, No. 8, August 1970, pp. 1523-1525. doi: 10.2514/3.5939

[3] Schaub, H., and Junkins J.L., *Analytical Mechanics of Space Systems*, AIAA Education Series, 2nd Edition, 2009.

[4] Lappas, V.J., Asghar, S., Palmer, P.L., and Fertin, D., *Combined Singularity Avoidance for Redundant Control Moment Gyro Clusters*, AIAA Guidance, Navigation and Control Conference and Exhibit, August 2004. doi: 10.2514/6.2004-5131

[5] Schaub, H. and Junkins, J.L., *CMG Singularity Avoidance Using VSCMG Null Motion*, AIAA/AAS Astrodynamics Specialist Conference and Exhibit, 1998. doi: 10.2514/6.1998-4388

[6] Leve, F.A., Boyarko, G.A., and Fitz-Coy, N.G., *Optimization in Choosing Gimbal Axis Orientations of a CMG Attitude Control System*, AIAA infotech@Aerospace Conference, 2009, 10.2514/6.2009-1836.

[7] Bayard, D.S., *An Optimization Result with Application to Optimal Spacecraft Reaction Wheel Orientation Design*, Proceedings of the American Control Conference, pp. 1473-1478.

[8] Blenden, R. and Schaub, H., *Regenerative Power-Optimal Reaction Wheel Attitude Control* Journal of Guidance, Control and Dynamics, Vol. 35, No. 4, July-August 2012, pp. 1208-1217. doi: 10.2514/1.55493

[9] Grassi, M. and Pastena, M., *Minimum Power Optimum Control of Microsatellite Attitude Dynamics*, Journal of Guidance, Control and Dynamics, Vol. 23, No. 5, Sept.-Oct. 2000, 10.2514/2.4640.

[10] Stevenson, D. and Schaub, H., *Nonlinear Control Analysis of a Double-Gimbal Variable Speed Control Moment Gyroscope*, Journal of Guidance, Control and Dynamics, Vol. 35, No. 3, May-June 2012. doi:10.2514/1.56104

[11] Schaub, H. and Lappas, V.J., *Redundant Reaction Wheel Torque Distribution Yielding Instantaneous L_2 Power-Optimal Attitude Control*, Journal of Guidance, Control, and Dynamics, Vol. 32, No.4, Aug. 2009.

[12] Lappas, V.J., Steyn, W.H., and Underwood, C., *Design and Testing of a Control Moment Gyroscope Cluster for Small Satellites*, Journal of Spacecraft and Rockets, Vol. 42, No. 4, July-Aug. 2005, pp. 729 - 739. doi:10.2514/1.7308

[13] Richie, D.J., Lappas, V.J., and Palmer, P.L., *Sizing/Optimization of a Small Satellite Energy Storage and Attitude Control System*, Journal of Spacecraft and Rockets, Vol. 44, No. 4, 2007, pp. 940-952. doi:10.2514/1.25134

[14] Carpenter, M.D., *Power-Optimal Steering of a Space Robotic System Driven by Control-Moment Gyroscopes*, AIAA Guidance, Navigation and Control Conference and Exhibit, 2008, 10.2514/6.2008-7270.

[15] LaSalle, J. and Lefschetz, S., *Stability by Lyapunov's Direct Method with Applications*, Academic Press, New York, NY, 1961.

[16] Mukherjee, R. and Chen, D., *Asymptotic Stability Theorem for Autonomous Systems*, Journal of Guidance, Control, and Dynamics, Vol. 16, September 1993, pp. 961-963.

[17] Kuhn, H.W. and Tucker, A.W., *Nonlinear Programming*, Proceedings of the Second Berkeley Symposium on Mathematical Statistics and Probability, pp. 481-492, University of California Press, Berkeley, CA, 1951.

[18] Press, W.H., Flannery, B.P., Teukolsky, S.A., and Vetterling, W.T., *Numerical Recipes in Fortran 77: The Art of Scientific Computing*, Cambridge University Press, 2nd Edition, 1992.